Published in final edited form as:
Anticancer Agents Med Chem. 2014 February ; 14(2): 204–210.

CCL21 and IFNγ Recruit and Activate Tumor Specific T cells in 3D Scaffold Model of Breast Cancer

Vy Phan-Lai[a,b], **Forrest M. Kievit**[b], **Stephen J. Florczyk**[b], **Kui Wang**[b], **Mary L. Disis**[a], and **Miqin Zhang**[b,*]

[a]Department of Medicine, University of Washington, Seattle, Washington 98109

[b]Department of Materials Science & Engineering, University of Washington, Seattle, Washington 98195

Abstract

Effective elicitation of endogenous immunity is associated with improved prognosis for cancer patients. Clinical evidence in hematological and solid cancers show that intratumoral injection of immunostimulatory genes primes and augments endogenous T cell responses. The ability of pro-inflammatory chemokines/cytokines to facilitate migration/activation of antigen-presenting cells (APC) and lymphocytes prompted our modeling of intratumoral delivery of a chemokine/cytokine combination for breast cancer treatment. Here, we demonstrate that expression of chemokine ligand 21 (CCL21) and interferon gamma (IFNγ) in tumors improves tumor specific T cell recruitment to tumor and activation in the tumor milieu. IFNγ and CCL21 were delivered into tumor cells via plasmids, and transfected cells were seeded to form spheroids on three-dimensional (3D) chitosan-alginate (CA) scaffolds. Co-expression of CCL21 and IFNγ, as evidenced by qRT-PCR and ELISA, induced increased recruitment, binding, and infiltration of anti-*neu* (p98) peptide specific T cells into the breast tumors as determined by SEM and immunofluorescence assays. The co-expression promoted recruitment of only p98 T cells, but not naïve T cells, demonstrating an antigen-restricted activation. Furthermore, the co-expression impacted T helper (Th) cell immunity, promoting an increase in secretion of pro-inflammatory Th-associated cytokine, tumor necrosis factor alpha (TNFα), and cytotoxic T lymphocyte (CTL)-associated protease, Granzyme B (GzB). Therefore, 3D CA scaffolds may be a useful breast cancer tumor microenvironment model to evaluate T cell function. Further characterization of CCL21-IFNγ mediated anti-tumor immunity will potentially benefit the development of chemokine/cytokine combination platforms as anti-cancer agents.

Keywords

Chemokines; Cytokines; Immunotherapy; Intratumoral; Microenvironment; Scaffolds; T lymphocytes

*Corresponding author: Department of Materials Science and Engineering, University of Washington, 302L Roberts Hall, Box 352120, Seattle, WA, 98195, USA. Telephone: 206-616-9356; Fax: 206-543-3100; mzhang@u.washington.edu. .

Conflict of Interest: none

INTRODUCTION

Tumor-antigen specific T cells are detectable in cancer patients, demonstrating that the immune system is capable of tumor recognition [1-2]. However, the tumor microenvironment can suppress the efficacy of standard and immune-based therapies [3-5]. Major factors which limit therapeutic efficacy and correlate to poor prognosis include sub-optimal presentation and priming by antigen-presenting cells (APCs) and poor T cell homing and infiltration into tumors because of stromal barriers [1, 5-6]. Endogenous anti-tumor immunity can be augmented if the local tumor microenvironment is modulated to favor a pro-inflammatory environment, promote dendritic cell (DC) activation, and support T cell function [6]. Chemokine and cytokine signals in the tumor microenvironment can facilitate immune cell migration and activation. We hypothesized that intratumoral over-expression of a chemokine/cytokine combination could promote a tumor microenvironment permissive to T cell homing and anti-tumor reactivity. Intratumoral delivery has been established as a potent strategy to deliver immunostimulatory genes and immune cells to elicit tumor regression [7-10].

Interferon gamma (IFNγ) and secondary lymphoid-tissue chemokine/chemokine ligand 21 (SLC/CCL21) are molecules with potent immunostimulatory activity. IFNγ is a cytokine secreted predominantly by Th1 cells that activates effector adaptive immune cells, promoting an anti-tumorigenic, pro-inflammatory tumor microenvironment. Thus, local IFNγ secretion at the tumor microenvironment represents a potentially effective strategy to modulate endogenous immunity [11]. IFNγ upregulates major histocompatibility complex class I (MHCI), which correlates with tumor inhibition, and major histocompatibility complex class II (MHCII) antigens on target cells, permitting enhanced antigen presentation [11-13]. Intratumoral administration of IFNγ has been shown to remodel the tumor environment, leading to reduced angiogenesis and normalization of the tumor vasculature [14-15]. Studies in colorectal cancer patients demonstrated that an IFNγ gene signature is a predictor of positive outcome [1, 16]. Furthermore, IFNγ production by T cells aids in targeting of stromal cells through IFNγ receptor binding and targeting of antigen loss variants to elicit complete elimination of tumors [17-19].

CCL21 directs immune effector cell migration to sites of pathological injury during infection and inflammation. In cancer, exposure to CCL21 and antigens presented by APCs can induce robust T cell activation, promoting cell-mediated immunity needed to control cancer cell growth. CCL21 has also been evaluated as a potent immune stimulator. Plasmid mediated delivery of CCL21, along with co-expression of human epidermal growth factor receptor 2/neu (Her2/neu) and granulocyte-macrophage colony-stimulating factor (GM-CSF), in breast cancer induced a Th1-polarized immunity, favorable for tumor rejection, and led to significant protection by the DNA vaccine (70% tumor-free mice) [20]. Genetic modification of *ex vivo* generated DCs to express CCL21, via adenoviral transduction, stimulates potent anti-tumor responses in murine models by augmenting tumor antigen presentation and T cell activation [21].

We generated an *in vitro* murine model of breast cancer using a 3D chitosan-alginate polyelectrolyte complex (CA) scaffold. 3D models have been applied for target validation,

drug testing, and patient selection for clinical trials, serving as an *in vivo*-like model for therapeutic translational studies [22]. We have tested CA scaffolds for the culture and renewal of stem cells and tumor cells [23-25] and previously demonstrated that CA scaffolds have high porosity and improved mechanical and biological properties over other scaffolds [26-27]. Here, we investigated how the over-expression of CCL21 and IFNγ in tumor cells grown in CA scaffolds affects T cell recruitment and infiltration into breast cancer tumor spheres. T cell recruitment into the scaffold and tumor spheres was determined by confocal microscopy. The effects of CCL21 and IFNγ expression in the tumor spheres on T cell activation were monitored through TNFα and CTL-associated protease, GzB, ELISAs. While preliminary, our studies on CCL21-IFNγ combination gene therapy show promise and provide rationale for further development of this therapeutic approach for breast cancer and potentially other solid cancers.

MATERIALS AND METHODS

Cell Culture and Transfection

The murine mammary carcinoma (MMC) cell line and p98 neu T cell line were derived from neu-transgenic (neu-Tg) mice [28]. MMC cells were cultured at 37°C in a 5% CO_2 humidified incubator in 1X RPMI medium supplemented with 10% FBS and 1% Penicillin/Streptomycin (Invitrogen, Carlsbad, CA), as previously described [28]. Mouse neu p98 (i.e. p98-114) specific T cells were isolated from splenocytes of p98-immunized *neu*-transgenic mice [FVB/N-TgN(MMTV$_{neu}$)-202Mul] (designated Tg-MMTV$_{neu}$), and maintained in 1X RPMI medium (Invitrogen Corporation, Carlsbad, CA) supplemented with 10% FBS (Invitrogen), 1% Penicillin/Streptomycin, and 50 μM β-mercaptoethanol (Sigma-Aldrich Corp., St. Louis, MO). MMC cells were transiently transfected using Lipofectamine 2000 reagent (Invitrogen), according to the manufacturer's instructions, with 1 μg of pDream2.1 vector (GenScript USA Inc., Piscataway, NJ) encoding mouse CCL21b (GenBank accession #: NM_011335) or encoding mouse IFNγ (GenBank accession #: NM_008337). Conditions included: CCL21 alone, IFNγ alone, or CCL21-IFNγ together; Red Fluorescent Protein (RFP) was used as the control.

Quantitative RT-PCR

mRNA expression of CCL21 or IFNγ (normalized to β-actin) was assessed three days after transfection by quantitative reverse transcriptase-PCR (qRT-PCR). For this, total RNA was extracted from MMC cells using the Qiagen RNeasy kit (Qiagen, Valencia, CA). cDNA was synthesized from 1 μg of the total RNA by extension with oligo (dT)18 primer and SuperScript II (Gibco BRL, Gaithersburg, MD, USA), according to the manufacturer's instructions. Mouse IFNγ or CCL21 genes were amplified by quantitative RT-PCR, in a 25 μl reaction using 4 pg cDNA as the template, SYBR Green PCR Master mix (Bio-Rad, Hercules, CA) for template amplification, and 0.2 μM of the following primers (Integrated DNA Technologies): IFNγ (PrimerBank ID #33468859a1): Forward, 5′-ATGAACGCTACACACTGCATC-3′ and Reverse, 5′-CCATCCTTTTGCCAGTTCCTC-3′; CCL21b (PrimerBank ID #14547891a1): Forward, 5′-GTGATGGAGGGGGTCAGGA-3′ and Reverse, 5′-GGGATGGGACAGCCTAAACT-3′, and β-actin (PrimerBank ID #142343868b1): Forward, 5′-

CAGCTCAGGCCGGGAATAC-3′ and Reverse, 5′-GCCTCCGAGATTGGCTGTG-3′. β-actin was run as a control to normalize IFNγ or CCL21 gene expression. The reactions were run in a Bio-Rad CFX96 real-time PCR detection machine under the following conditions: 95°C for 15 min, 45 cycles of denaturation (15 s, 94°C), annealing (30 s, 55°C), and extension (30 s, 72°C). The expression of gene expression normalized to β-actin was calculated from Ct (cycling threshold) values, using the formula: $2^{[(Ct_{\text{gene of interest}} - Ct_{\beta\text{-actin}})]}$. Triplicates of each sample were run in two experiments.

Enzyme-Linked Immunosorbent Assay (ELISA)

Supernatants (1 ml) from cell cultures were collected three days after tumor transfection or three days after tumor/T-cell co-culture and stored at −80°C. Quantification of CCL21 (R&D), IFNγ (eBioscience), TNFα (eBioscience), or GzB (eBioscience) were performed by ELISA, according to the manufacturer's instructions for each. Experiments were repeated twice, with each sample assayed in minimum triplicate wells. Cytokine concentrations are reported in pg/ml.

CA Scaffold Synthesis and Cell Seeding and Dissociation

3D CA scaffolds were generated as previously described [23]. In brief, 4 wt% CA scaffolds were prepared using a mixture of 4 wt% chitosan solution and 4 wt% alginate solution, and cast in molds. After incubation at 4°C for 12 hours and −20°C overnight, the scaffolds were lyophilized and sectioned into 2 mm thick, 13 mm diameter discs. MMC cells were collected three days after transfection and gently transferred onto scaffolds in 100 μl complete media per sample, either directly in 12-well plate wells (2D) or on top of 3D CA scaffolds placed inside 12-well plates. The samples were incubated at 37°C and 5% CO_2 in a fully humidified incubator for 1.5 hours before 2 ml fully supplemented media was added to each well. T cells (5×10^6) were seeded onto scaffolds 24 hours after MMC seeding on scaffolds. Cells were dissociated from scaffolds using 1X Versene (Invitrogen), as previously described [24-25]. In brief, 1.5 ml of 1X Versene in PBS was added per well for 30 min at 37°C. Cells were gently dissociated from scaffolds with additional mechanical disruption by pressing scaffolds gently using forceps.

Preparation of Scaffolds for Confocal Immunofluorescence Microscopy

T cells and tumor cells were prepared three days after co-culture experiments. Cells were prepared for confocal fluorescence imaging in one of two ways. For T cell binding to the tumor surface, tumor scaffolds (cultured with and without Green Cell Tracker-labeled T cells) were fixed with 4% formaldehyde in PBS for 30 min, and transferred to 110 mm diameter Petri dishes customized for confocal microscopy (part of the dish bottom was removed and replaced with a coverslip for viewing). Media was added to the Petri dish to cover the scaffolds and keep the cells viable. The samples were imaged with a confocal laser scanning microscope (Zeiss 510 META LSM, Carl Zeiss AG, Oberkochen, Germany).

For T cell infiltration, the tumor scaffolds were fixed as above, and embedded in OCT cryo-compound (Fisher Scientific, Waltham, MA) in cryomolds (Fisher Scientific), and allowed to freeze on dry ice. The frozen blocks were cut into 15 μm sections and mounted onto glass

slides. Slides were mounted with Prolong Gold Antifade reagent containing DAPI (Fisher Scientific). Cells were imaged on the confocal laser scanning microscope.

SEM Imaging

Samples for scanning electron microscopy (SEM) analysis were fixed with 2.5% glutaraldehyde in fully supplemented media for 30 minutes at 37°C. The samples were then fixed in 2.5% glutaraldehyde in 0.1 M sodium cacodylate buffer overnight at 4°C. The samples were dehydrated in a series of ethanol washes (0%, 30%, 50%, 70%, 85%, 95%, 100%), with each wash performed twice. The samples were critical point dried, sectioned, mounted, and sputter coated with platinum, then imaged with a JSM-7000F SEM (JEOL, Tokyo, Japan).

RESULTS

Transfection of CCL21 and IFNγ Genes in MMCs Promote the Cytokine/Chemokine Expression

Murine breast cancer cells were established in 3D culture, *in vitro*, by seeding onto a CA scaffold, which provides an extracellular matrix, preserves *in vivo*-like phenotype and function, and mimics the breast tumor microenvironment for cell-cell interaction studies. Using this *in vitro* 3D breast tumor model, we questioned if over-expression of CCL21 and IFNγ in the tumor, via plasmid-mediated delivery, could augment lymphocytic recruitment and infiltration into tumor and/or promote tumor specific T cell activation. There was significant up-regulation of CCL21 mRNA and IFNγ mRNA in the cells transfected with the respective plasmids. CCL21 mRNA levels normalized to β-actin (mean ± SD) in MMC-RFP, MMC-CCL21, MMC-IFNγ and MMC-CCL21-IFNγ were: 0.0018 ± 0.0002, 0.8452 ± 0.0655, 0.0027 ± 0.0003, and 1.97 ± 0.11, respectively (Figure 1a). Therefore, compared to RFP there was a significant up-regulation of CCL21 mRNA in MMC-CCL21 (470-fold increase) and in MMC-CCL21-IFNγ (1094-fold increase) (Figure 1a). The expression levels of IFNγ (mean + SD) in MMC-RFP, MMC-CCL21, MMC-IFNγ and MMC-CCL21-IFNγ were: 0.0004 ± 0.0001, 0.0002 ± 0.0000, 3.76 ± 0.34, and 1.48 ± 0.087, respectively (Figure 1b). Thus, compared to RFP, there was a significant upregulation of IFNγ transcript in MMC-IFNγ (9392-fold increase) and in MMC-CCL21-IFNγ (3700-fold increase) (Figure 1b). Furthermore, as expected, transfection of CCL21 did not increase IFNγ levels, and vice versa.

Confirmation of CCL21 and IFNγ protein secretions were assessed by ELISAs 3–4 days after transfection. There were detectable basal levels of CCL21 from RFP-transfected and IFNγ transfected cells, 50.5 ± 5.5 pg/ml and 76.6 ± 3.9 pg/ml, respectively (Figure 1c). However, a significant up-regulation of secreted CCL21 was detected by MMC-CCL21 (221.5 ± 5.6 pg/ml) and by MMC-CCL21-IFNγ cells (213.8 ± 11.3 pg/ml) (Figure 1c). For IFNγ, there was no detectable IFNγ expression in MMC-RFP cells (0.0 ± 0.1 pg/ml), compared to a significant upregulation in MMC-IFNγ cells (85.8 ± 10.0 pg/ml) and MMC-CCL21-IFNγ cells (96.5 ± 14.0 pg/ml) (Figure 1d).

Co-Expression of CCL21 and IFNγ Elicits Antigen-Specific T Cell Infiltration

The observed increase in T cell binding to MMC-CCL21-IFNγ scaffolds prompted the evaluation of T cell binding (Figure 2a) and infiltration into scaffolds (Figure 2b) by confocal microscopy. Figure 2a shows a representative image of T cells bound to MMC cells in the scaffold. The Green Cell Tracker labeled T cells were clearly discernible (solid white arrow) from the porous scaffold matrices (dashed white arrow) and MMC cells (outlined by the red membrane dye) in the scaffold cross section (Figure 2a). The cells localized within the pores of the scaffolds, as previously observed using scanning electron microscopy (SEM) [29] .

Figure 2b shows a representation of T cell binding in the scaffold interior. Here again, labeled T cells (solid white arrow) were clearly discernible and found clustered together, within the scaffold matrix (dashed white arrow). Among the tumor scaffolds (MMC-RFP, MMC-CCL21, MMC-IFNγ, or MMC-CCL21-IFNγ cells), we observed that MMC-CCL21-IFNγ scaffolds contained an increased number of labeled T cells. Quantification of the percent of T cells adhering to the scaffolds was performed for ten random fields of view (FOV) (Figure 2c). The mean ± SD number of T cells that bound to empty scaffolds or scaffolds seeded with MMC, MMC-RFP, MMC-CCL21, MMC-IFNγ, and MMC-CCL21-IFNγ were: 8.0 ± 2.4, 6.9 ± 1.9, 7.9 ± 2.6, 11.5 ± 3.9, 10.3 ± 5.3, and 30.9 ± 8.5, respectively (Figure 2c). Thus, there was a much higher T cell attachment in MMC-CCL21-IFNγ scaffolds as compared to each of the other conditions. To assess if the binding to MMC-CCL21-IFNγ cells was antigen-restricted, naïve T cells were co-cultured with the tumor scaffolds. The mean ± SD number of T cells which bound to empty scaffolds or scaffolds seeded with MMC, MMCRFP, MMC-CCL21, MMC-IFNγ, and MMC-CCL21-IFNγ were: 6.8 ± 2.2, 4.8 ± 1.5, 4.1 ± 1.7, 5.1 ± 1.1, 3.0 ± 1.8, and 7.0 ± 4.4, respectively (Figure 2d). Naive T cell binding to MMC-CCL21-IFNγ cells was not different as compared to the other conditions.

To further confirm the effect of combined CCL21-IFNγ on T cell accumulation and recruitment, T cells were cultured for three days with the various MMC-seeded scaffolds and imaged using SEM. T cells could be seen attached to MMC cells in the scaffold (Figure 3).

Co-Expression of CCL21 and IFNγ Promotes Pre-primed T Cell Response

We hypothesized that induction of CCL21 and particularly, IFNγ, would augment T cell activation. To address this, we assessed the ability of the antigen specific T cells to secrete activation-associated cytokines, e.g. GzB (CTL-associated) and TNFα (Th1-associated), after co-culture with CCL21 and/or IFNγ transfected tumor cells. In the absence of T cells, there was no to low levels of GzB and TNFα (Figure 4a, d). GzB production by T cells was not greatly increased in MMC-CCL21-IFNγ scaffolds as compared to each of the other conditions (Figure 4b). Furthermore, TFNα production was increased when cultured with MMCCCL21-IFNγ cells, but showed no combined effect with IFNγ. Co-culture of naïve T cells with MMC-CCL21-IFNγ cells, compared to MMC or MMC-RFP, did not show alteration in GzB (Figure 4c) nor TNFα production (Figure 4f).

DISCUSSION

In vitro models to study tumor-immune cell interactions have been limited. Here, we evaluated tumor-T cell interactions through culture on biomaterial scaffolds. These scaffolds, comprised of chitosan and alginate, have been used in our laboratory for various tumor microenvironment applications [23-25]. We have recently documented the use of CA scaffolds compared to 2D culture systems for the culture of breast cancer cells [29]. We demonstrated that CA scaffolds support productive cell growth and formation of distinct tumor spheroids, and the cells (T cells, tumor cells) seeded on the scaffolds are allowed to interact in 3D, representing a more 'in-vivo' like model of respective cell-cell interaction in the breast tumor environment [29]. Chemokines and cytokines play key roles in the initiation of effective antitumor immune responses – chemokines can direct lymphocytic migration while cytokines can direct the polarization and activation of APCs (e.g. DC, macrophages) and T cells. Our hypothesis was that intratumoral expression of a pro-inflammatory cytokine (IFNγ) and chemokine (CCL21) in breast tumor cells could augment T cell migration to tumor cells while simultaneously activating endogenous T cell function.

In this study, we demonstrated that CCL21 or IFNγ, as solo agents, are not as effective as they are in combination. When combined, the molecules synergized to promote tumor specific T cell binding (Figure 2, Figure 3a), infiltration (Figure 3b-d), and pre-primed T cell activity (Figure 4) in the tumor microenvironment. Thus, acting in concert, both molecules were capable of augmenting adaptive immunity in the local tumor microenvironment. Gene transfer was accomplished by endogenous expression of CCL21 and IFNγ. Other means of gene transfer, including nanoparticles [30] and viruses [31] have been evaluated and are warranted for future studies to potentially increase expression of CCL21 and IFNγ. Nonetheless, plasmid-mediated delivery (lipofection) of CCL21 and IFNγ induced a robust up-regulation of the respective transcripts (Figure 1a, b) and a significant up-regulation in the respective proteins (Figure 1c, d).

Confocal microscopy was used to evaluate T cell binding and infiltration in tumor scaffolds (Figure 2). Since T cell to tumor cell ratio in co-culture was 100:1 (based on E:T ratio determined to be most suitable for T cell activity[29]), the T cells appeared in greater abundance (Figure 2b). Fluorescent staining revealed the T cells (DAPI+, green+) clustering on top of tumor cells (DAPI+, green-) (Figure 2b). The fact that T cells and tumor cells are found in the same plane, in 3D, indicates that they are capable of interacting with each other. Importantly, neu specific p98 T cells showed significantly increased infiltration into the MMC-CCL21-IFNγ scaffolds than the other tumor-seeded scaffolds (Figure 2c, d). Since T cell infiltration was not significant in MMC-CCL21 or MMC-IFNγ scaffolds compared to control scaffold (MMC-RFP), but only significant in combination scaffold, the results demonstrate that IFNγ and CCL21 synergized to mediate T cell recruitment and infiltration (Figure 2). Control T cells (naïve) did not bind or infiltrate into MMC-CCL21-IFNγ scaffolds (Figure 2d). Therefore, recruitment of adaptive effector T cells is tumor-antigen restricted. Moreover, while the production of CCL21 protein ranged only up to 200–250 pg/ml (Figure 1c), there appeared to be sufficient biological activity at this concentration, in combination with IFNγ, to exert an increase in T cell recruitment into tumors. SEM imaging confirmed attachment of the T cells to the MMC tumor spheres in the scaffolds (Figure 3).

In determining which subpopulation of T cells (Th or CTL) was predominantly responsive to CCL21-IFNγ, we assayed for TNFα and GzB secretion. TNFα is secreted by monocytes, macrophages, neutrophils, natural killer (NK) cells, and Th cells following activation, whereas CTL secrete little to no TNFα. GzB is a protease secreted only by CTL following activation, whereas Th cells secrete no GzB. CCL21-IFNγ co-expression significantly up-regulated production of GzB (Figure 4b) but not of TNFα (Figure 4e) by T cells. Though the tumor cells were not separated from T cells for this study, GzB or TNFα were mainly from T cells since supernatants from breast cancer cell cultures alone did not show detectable levels of GzB or TNFα. The effect of CTL activation (GzB) by CCL21-IFNγ was greatly increased as compared to the individual treatments, suggesting a synergistic role for CCL21 and IFNγ in CTL recruitment and activation. While TNFα production was also elicited by the combination CCL21-IFNγ therapy, CCL21 alone also showed an increase in TNFα production, highlighting the minimal role IFNγ plays in recruitment and activation of Th cells. Future studies involving more Th- and CTL-specific cytokines are needed to better discern how Th cells and CTL are impacted by CCL21-IFNγ signaling. The observation that CCL21-IFNγ induced activation appears to be tumor-antigen restricted (i.e., naïve T cells did not show alteration of GzB nor TNFα (Figure 4c, f)) would suggest that the combination is, indeed, impacting tumor specific T cell function. Furthermore, it is possible that while the combination enhances antigen specific T cell recruitment (Figure 2), T cell activation in the tumor may require more robust immunostimulatory signals to overcome the suppressive factors in the tumor milieu. Using the CA scaffold system, however, we have successfully demonstrated the ability to develop and test the benefits of a combinatorial chemokine/cytokine approach for tumor immunotherapy.

CONCLUSIONS

In conclusion, our data demonstrates that CA scaffolds can mimic the breast tumor microenvironment to enable studies of tumor-T cell interactions. A chemokine/cytokine combination, such as the CCL21-IFNγ combination described herein, may be employed as an effective anti-cancer strategy. We demonstrated that the combination can promote T cell recruitment into the tumor microenvironment, and may enhance the immune response by pre-primed T cells. Further development of these preliminary findings on CCL21-IFNγ combination may lead to a new and promising therapy for breast cancer and other cancers.

Acknowledgments

This work was supported in part by NIH grants R01CA134213 and R01EB006043, and a Kyocera Professorship Endowment to M.Z, and R01CA136632 to M.L.D. V.P.L. and F.M.K. acknowledge support through the Ruth L. Kirschstein NIH Training grant T32 CA138312 and V.P.L. through the DOD Breast Cancer Research Program Multidisciplinary Postdoctoral Award W81XWH-06-1-0724. S.J.F acknowledges support through Egtvedt Scholarship funding. We thank the Materials Science and Engineering Electron Microscopy facility, the Keck Center Confocal Microscopy facility, and the Histology Core for use of resources.

List of Abbreviations

3D	three-dimensional
APC	antigen-presenting cells

CA	chitosan-alginate
CCL21	chemokine ligand 21
CTL	cytotoxic T lymphocyte
ELISA	enzyme-linked immunosorbant assay
IFNγ	interferon-gamma
GM-CSF	granulocyte-macrophage colony-stimulating factor
GzB	Granzyme B
HER2/neu	human epidermal growth factor receptor 2/neu
MHCI	major histocompatibility complex class I
MHCII	major histocompatibility complex class II
MMC	murine mammary carcinoma
NK	natural killer
neu-Tg	neu-transgenic
qRT-PCR	quantitative reverse transcriptase-PCR
RFP	red fluorescent protein
SEM	scanning electron microscopy
SLC	secondary lymphoid-tissue chemokine
Th	T helper
Th1	T helper 1
TNFα	tumor necrosis factor alpha

REFERENCES

[1]. Galon J, Costes A, Sanchez-Cabo F, Kirilovsky A, Mlecnik B, Lagorce-Pages C, Tosolini M, Camus M, Berger A, Wind P, Zinzindohoue F, Bruneval P, Cugnenc PH, Trajanoski Z, Fridman WH, Pages F. Type, density, and location of immune cells within human colorectal tumors predict clinical outcome. Science. 2006; 313(5795):1960–4. [PubMed: 17008531]

[2]. Zhang L, Conejo-Garcia JR, Katsaros D, Gimotty PA, Massobrio M, Regnani G, Makrigiannakis A, Gray H, Schlienger K, Liebman MN, Rubin SC, Coukos G. Intratumoral T cells, recurrence, and survival in epithelial ovarian cancer. N Engl J Med. 2003; 348(3):203–13. [PubMed: 12529460]

[3]. Apetoh L, Ghiringhelli F, Tesniere A, Obeid M, Ortiz C, Criollo A, Mignot G, Maiuri MC, Ullrich E, Saulnier P, Yang H, Amigorena S, Ryffel B, Barrat FJ, Saftig P, Levi F, Lidereau R, Nogues C, Mira JP, Chompret A, Joulin V, Clavel-Chapelon F, Bourhis J, Andre F, Delaloge S, Tursz T, Kroemer G, Zitvogel L. Toll-like receptor 4-dependent contribution of the immune system to anticancer chemotherapy and radiotherapy. Nat Med. 2007; 13(9):1050–9. [PubMed: 17704786]

[4]. Rabinovich GA, Gabrilovich D, Sotomayor EM. Immunosuppressive strategies that are mediated by tumor cells. Annu Rev Immunol. 2007; 25:267–96. [PubMed: 17134371]

[5]. Phan V, Disis ML. Tumor stromal barriers to the success of adoptive T cell therapy. Cancer Immunol Immunother. 2008; 57(2):281–3. [PubMed: 17646987]

[6]. Kaufman HL, Disis ML. Immune system versus tumor: shifting the balance in favor of DCs and effective immunity. J Clin Invest. 2004; 113(5):664–7. [PubMed: 14991063]

[7]. Houot R, Levy R. T-cell modulation combined with intratumoral CpG cures lymphoma in a mouse model without the need for chemotherapy. Blood. 2009; 113(15):3546–52. [PubMed: 18941113]

[8]. Kim YH, Gratzinger D, Harrison C, Brody JD, Czerwinski DK, Ai WZ, Morales A, Abdulla F, Xing L, Navi D, Tibshirani RJ, Advani RH, Lingala B, Shah S, Hoppe RT, Levy R. In situ vaccination against mycosis fungoides by intratumoral injection of a TLR9 agonist combined with radiation: a phase 1/2 study. Blood. 2012; 119(2):355–63. [PubMed: 22045986]

[9]. Kaufman HL, Deraffele G, Mitcham J, Moroziewicz D, Cohen SM, Hurst-Wicker KS, Cheung K, Lee DS, Divito J, Voulo M, Donovan J, Dolan K, Manson K, Panicali D, Wang E, Horig H, Marincola FM. Targeting the local tumor microenvironment with vaccinia virus expressing B7.1 for the treatment of melanoma. J Clin Invest. 2005; 115(7):1903–12. [PubMed: 15937544]

[10]. Kaufman HL, Cohen S, Cheung K, DeRaffele G, Mitcham J, Moroziewicz D, Schlom J, Hesdorffer C. Local delivery of vaccinia virus expressing multiple costimulatory molecules for the treatment of established tumors. Hum Gene Ther. 2006; 17(2):239–44. [PubMed: 16454657]

[11]. Shankaran V, Ikeda H, Bruce AT, White JM, Swanson PE, Old LJ, Schreiber RD. IFNgamma and lymphocytes prevent primary tumour development and shape tumour immunogenicity. Nature. 2001; 410(6832):1107–11. [PubMed: 11323675]

[12]. Panelli MC, Wang E, Shen S, Schluter SF, Bernstein RM, Hersh EM, Stopeck A, Gangavalli R, Barber J, Jolly D, Akporiaye ET. Interferon gamma (IFNgamma) gene transfer of an EMT6 tumor that is poorly responsive to IFNgamma stimulation: increase in tumor immunogenicity is accompanied by induction of a mouse class II transactivator and class II MHC. Cancer Immunol Immunother. 1996; 42(2):99–107. [PubMed: 8620527]

[13]. Matory YL, Chen M, Dorfman DM, Williams A, Goedegebuure PS, Eberlein TJ. Antitumor activity of three mouse mammary cancer cell lines after interferon-gamma gene transfection. Surgery. 1995; 118(2):251–5. discussion 255-6. [PubMed: 7638741]

[14]. Ganss R, Ryschich E, Klar E, Arnold B, Hammerling GJ. Combination of T-cell therapy and trigger of inflammation induces remodeling of the vasculature and tumor eradication. Cancer Res. 2002; 62(5):1462–70. [PubMed: 11888921]

[15]. Goel S, Duda DG, Xu L, Munn LL, Boucher Y, Fukumura D, Jain RK. Normalization of the vasculature for treatment of cancer and other diseases. Physiological reviews. 2011; 91(3):1071–121. [PubMed: 21742796]

[16]. Camus M, Tosolini M, Mlecnik B, Pages F, Kirilovsky A, Berger A, Costes A, Bindea G, Charoentong P, Bruneval P, Trajanoski Z, Fridman WH, Galon J. Coordination of intratumoral immune reaction and human colorectal cancer recurrence. Cancer Res. 2009; 69(6):2685–93. [PubMed: 19258510]

[17]. Zhang B, Bowerman NA, Salama JK, Schmidt H, Spiotto MT, Schietinger A, Yu P, Fu YX, Weichselbaum RR, Rowley DA, Kranz DM, Schreiber H. Induced sensitization of tumor stroma leads to eradication of established cancer by T cells. J Exp Med. 2007; 204(1):49–55. [PubMed: 17210731]

[18]. Zhang B, Karrison T, Rowley DA, Schreiber H. IFN-gamma- and TNF-dependent bystander eradication of antigen-loss variants in established mouse cancers. J Clin Invest. 2008; 118(4): 1398–404. [PubMed: 18317595]

[19]. Spiotto MT, Rowley DA, Schreiber H. Bystander elimination of antigen loss variants in established tumors. Nat Med. 2004; 10(3):294–8. [PubMed: 14981514]

[20]. Nguyen-Hoai T, Baldenhofer G, Sayed Ahmed MS, Pham-Duc M, Vu MD, Lipp M, Dorken B, Pezzutto A, Westermann J. CCL21 (SLC) improves tumor protection by a DNA vaccine in a Her2/neu mouse tumor model. Cancer Gene Ther. 2012; 19(1):69–76. [PubMed: 21997231]

[21]. Riedl K, Baratelli F, Batra RK, Yang SC, Luo J, Escuadro B, Figlin R, Strieter R, Sharma S, Dubinett S. Overexpression of CCL-21/secondary lymphoid tissue chemokine in human dendritic cells augments chemotactic activities for lymphocytes and antigen presenting cells. Mol Cancer. 2003; 2:35. [PubMed: 14613584]

[22]. Lee GY, Kenny PA, Lee EH, Bissell MJ. Three-dimensional culture models of normal and malignant breast epithelial cells. Nat Methods. 2007; 4(4):359–65. [PubMed: 17396127]

[23]. Florczyk SJ, Kim DJ, Wood DL, Zhang M. Influence of processing parameters on pore structure of 3D porous chitosan-alginate polyelectrolyte complex scaffolds. J Biomed Mater Res A. 2011; 98(4):614–20. [PubMed: 21721118]

[24]. Kievit FM, Florczyk SJ, Leung MC, Veiseh O, Park JO, Disis ML, Zhang M. Chitosan-alginate 3D scaffolds as a mimic of the glioma tumor microenvironment. Biomaterials. 2010; 31(22): 5903–10. [PubMed: 20417555]

[25]. Leung M, Kievit FM, Florczyk SJ, Veiseh O, Wu J, Park JO, Zhang M. Chitosan-alginate scaffold culture system for hepatocellular carcinoma increases malignancy and drug resistance. Pharm Res. 2010; 27(9):1939–48. [PubMed: 20585843]

[26]. Li Z, Ramay HR, Hauch KD, Xiao D, Zhang M. Chitosan-alginate hybrid scaffolds for bone tissue engineering. Biomaterials. 2005; 26(18):3919–28. [PubMed: 15626439]

[27]. Li Z, Zhang M. Chitosan-alginate as scaffolding material for cartilage tissue engineering. J Biomed Mater Res A. 2005; 75(2):485–93. [PubMed: 16092113]

[28]. Lu H, Knutson KL, Gad E, Disis ML. The tumor antigen repertoire identified in tumor-bearing neu transgenic mice predicts human tumor antigens. Cancer Res. 2006; 66(19):9754–61. [PubMed: 17018635]

[29]. Phan-Lai V, Florczyk SJ, Kievit FM, Wang K, Gad E, Disis ML, Zhang M. Three-Dimensional Scaffolds to Evaluate Tumor Associated Fibroblast-Mediated Suppression of Breast Tumor Specific T Cells. Biomacromolecule. in press. DOI: 10.1021/bm301928u.

[30]. Kar UK, Srivastava MK, Andersson A, Baratelli F, Huang M, Kickhoefer VA, Dubinett SM, Rome LH, Sharma S. Novel CCL21-vault nanocapsule intratumoral delivery inhibits lung cancer growth. PLoS One. 2011; 6(5):e18758. [PubMed: 21559281]

[31]. Thanarajasingam U, Sanz L, Diaz R, Qiao J, Sanchez-Perez L, Kottke T, Thompson J, Chester J, Vile RG. Delivery of CCL21 to metastatic disease improves the efficacy of adoptive T-cell therapy. Cancer Res. 2007; 67(1):300–8. [PubMed: 17210711]

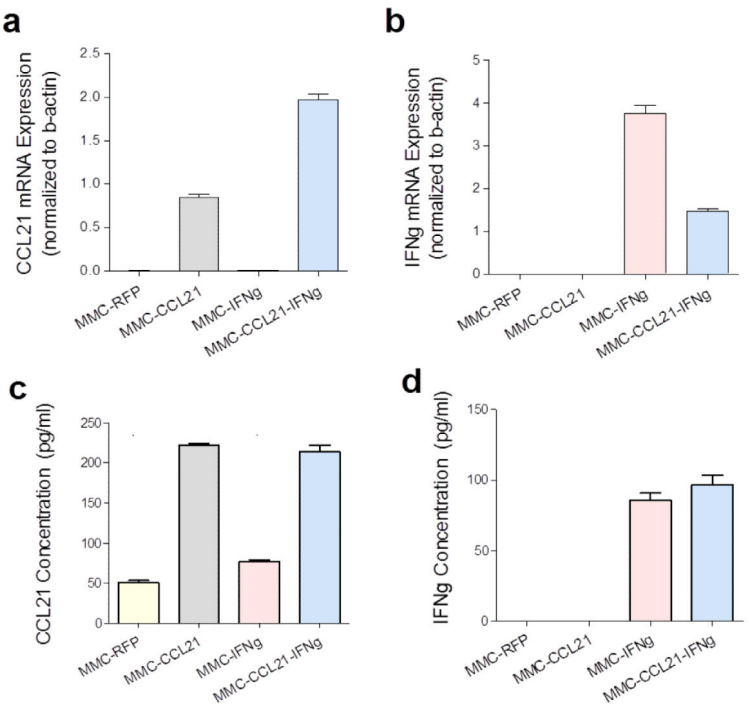

Figure 1. Analysis of CCL21 and IFNγ expression in transfected MMC breast cancer cells

(a, b) Expression of CCL21 or IFNγ mRNA, respectively. RNA extracted from MMC cells three days after plasmid transfection of RFP, CCL21, IFNγ, or dual CCL21-IFNγ. The transcript level of CCL21 or IFNγ was analyzed by qRT-PCR; β-actin was included as a control for normalization. **(c, d)** Secreted protein levels of CCL21 or IFNγ, respectively, from culture media of MMC cells three days after transfection by ELISA. Data shown is representative of two experiments.

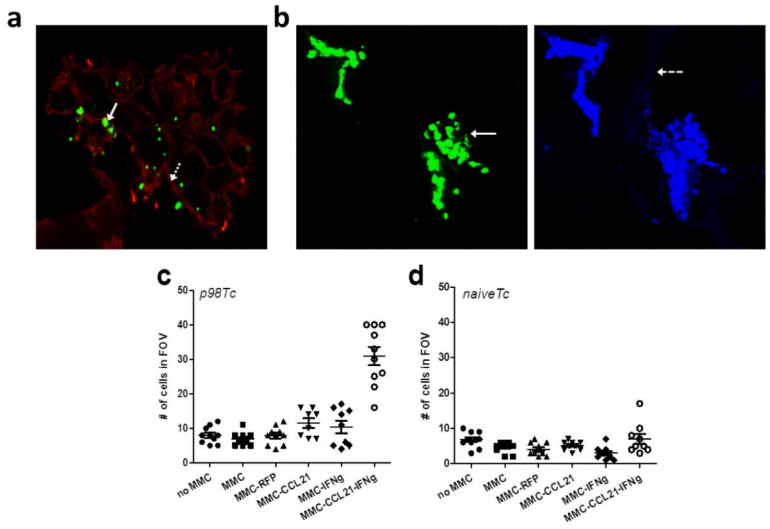

Figure 2. Detection and quantification of T cells on MMC tumor scaffolds

a) Confocal imaging of surface of a tumor scaffold after T cell-MMC co-culture. T cells (Cell Tracker green labeled; solid white arrow) shown binding within the MMC tumors (red membrane dye; dashed white arrow) in the scaffold. **b)** Confocal imaging of the interior (15 μm cross-section) of a tumor scaffold after T-cell-MMC co-culture (slide prepared from a frozen OCT-embedded scaffold block). T cells (Cell Tracker Green labeled, solid white arrow, with DAPI counterstain) were imaged at 630×; scaffold matrix (dashed white arrow). **(c, d)** Quantification of T cell binding to tumor scaffolds. Tumor scaffolds were cultured with p98T cells or naïve T cells, respectively. The cells in the field of view (FOV) from the interior of the scaffolds were quantified at 630× magnification and depicted in the scatterplot. Data is representative of two experiments.

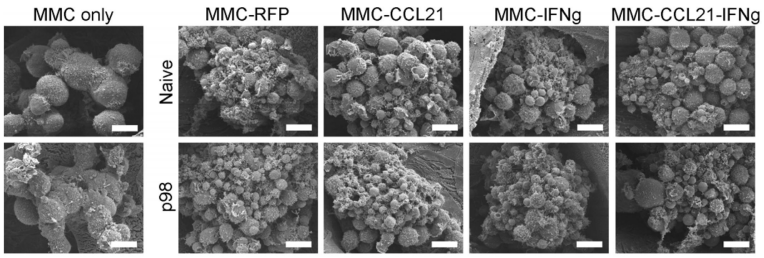

Figure 3. SEM images of bound p98 T cells on tumor scaffolds

T cells (p98 or naïve) were cultured with MMC-seeded scaffolds for three days prior to imaging with SEM. Scale bars correspond to 10 μm.

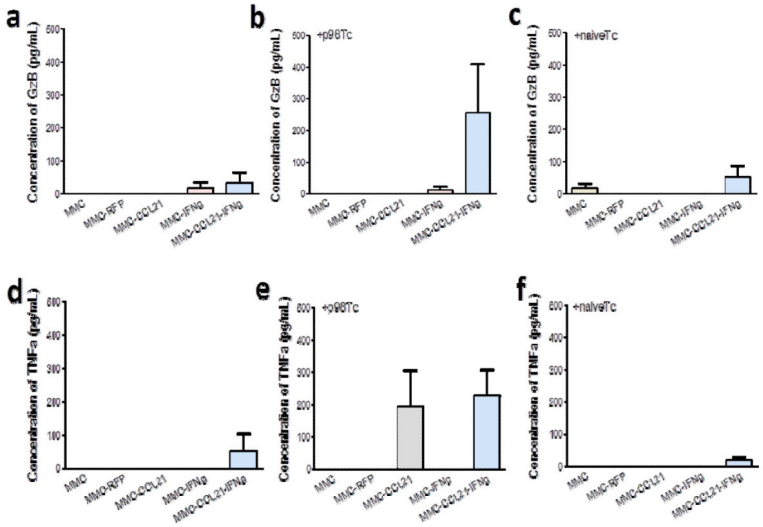

Figure 4. Analysis of CTL- and Th-associated cytokines from T cells co-cultured with transfected MMC breast cancer cells

Untreated MMC cells or cells transfected with RFP, CCL21, IFNγ, or CCL21 and IFNγ, were cultured in the absence or presence of p98 neu specific T cells or naïve T cells. (**a, b, c**) GzB (CTL-associated) production in the absence, or presence of p98 T cells or naïve T cells, respectively. (**d, e, f**) TNFα (Th1-associated) production in the absence, or presence of p98 T cells or naïve T cells, respectively. The y-axis depicts cytokine production in pg/ml. Data shown are from triplicate samples and representative of two experiments.